ISSN 1359-7345 • CHCOFS (15)1781-1971 (2003)

ChemComm

CHEMICAL COMMUNICATIONS • www.rsc.org/chemcomm

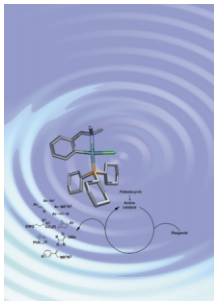

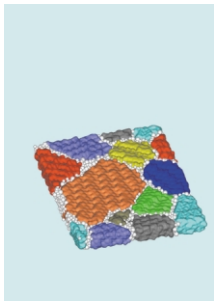

Cover (far left)
A palladacyclic pre-catalyst, and the range of C–C and C–heteroatom bond-forming reactions mediated by such pre-catalysts. Courtesy of Ann Bingham and Simon Coles of the EPSRC crystallography service, Southampton.

Inside cover (left)
A slice cut through a BaF_2 layer, depicting the nanopolycrystalline BaF_2.

contents

Chemical Communications
http://www.rsc.org/chemcomm

Chemical Communications (print: ISSN 1359-7345; electronic: ISSN 1364-548X) is published 24 times a year by the Royal Society of Chemistry, Thomas Graham House, Science Park, Milton Road, Cambridge, UK CB4 0WF. All orders accompanied by payment should be sent directly to Turpin Distribution Services Ltd, Blackhorse Road, Letchworth, Herts, UK SG6 1HN. 2003 Annual (print + electronic) subscription price: £878; US$1450. 2003 Annual (electronic) subscription price: £790; US$1305. Customers in Canada will be subject to a surcharge to cover GST. Customers in the EU subscribing to the electronic version only will be charged VAT. If you take an institutional subscription to any RSC journal you are entitled to free, site-wide web access to that journal. You can arrange access via Internet Protocol (IP) address at www.rsc.org/ip. Customers should make payments by cheque in sterling payable on a UK clearing bank or in US dollars payable on a US clearing bank. Periodicals postage paid at Rahway, NJ, USA and at additional mailing offices. Airfreight and mailing in the USA by Mercury Airfreight International Ltd., 365 Blair Road, Avenel, NJ 07001, USA. US Postmaster: send address changes to *Chemical Communications*, c/o Mercury Airfreight International Ltd., 365 Blair Road, Avenel, NJ 07001. All despatches outside the UK by Consolidated Airfreight.
PRINTED IN THE UK.

Advertisement sales: Tel +44 (0)1223 432243; Fax +44 (0)1223 426017; E-mail advertising@rsc.org

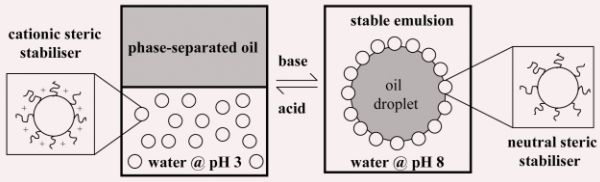

A pH-responsive, sterically-stabilised polystyrene latex is used as a particulate emulsifier for oil-in-water emulsions; demulsification occurs on lowering the solution pH and the emulsion is reformed on pH cycling.

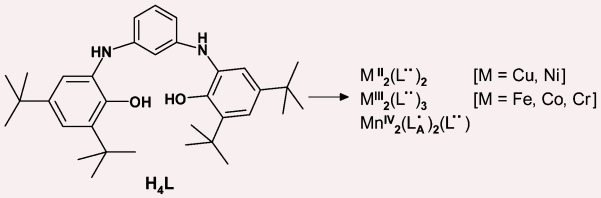

A series of dinuclear transition metal complexes with either *six* or *four* iminosemiquinone radicals, in which the metal centres are separated by a distance of ~6.8 Å, together with their catalytic reactivity is reported.

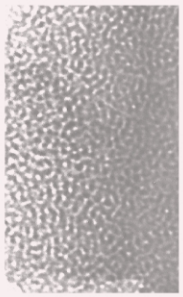

The beneficial effects that alkali metal and tetra-alkyl ammonium salt additions to molecularly templated silica sols have on the resulting mesoporous silica film are described. Films, formed from evaporative-coating methods, using the doped sols exhibited significant improvement in porosity, film surface uniformity, and dielectric constant.

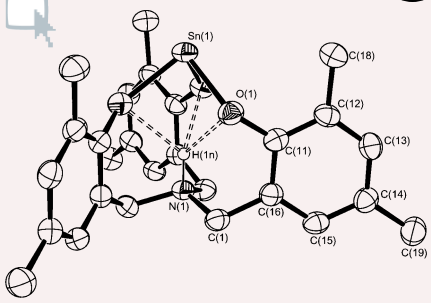

Reaction of $Zr(O^iPr)_4$ or $Sn[N(SiMe_3)_2]_2$ with the tris-phenol amine ligand $H_3L^{(Me/Me)}$ results in the formation of zirconium or tin complexes containing the new C_3-symmetric zwitterionic ammonium-trisphenolate ligand HL^{2-}.

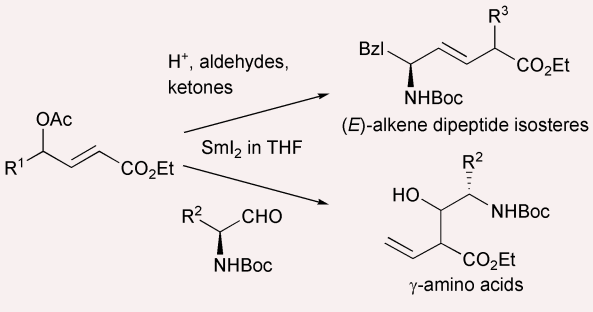

Samarium diiodide (SmI_2)-induced reductive formation of dienolates from γ-acetoxy-α,β-enoates followed by kinetic electrophilic trapping was successfully applied to the synthesis of various amino acid derivatives.

1836

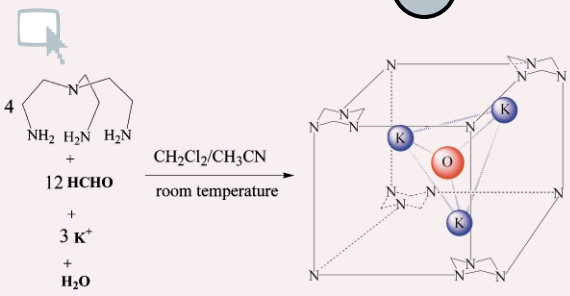

A novel pyramidal multiple alkali metal cluster $[K_3(H_2O)]^{3+}$ stabilized within a capsule containing 16-nitrogen donors

Zhang Bing-guang, Guo Dong, Duan Chun-ying,* Cai Ping and Meng Qing-jin*

A novel pyramidal multiple alkali metal cluster $[K_3(H_2O)]^{3+}$ stabilized within a capsule containing 16-nitrogen donors.

1838

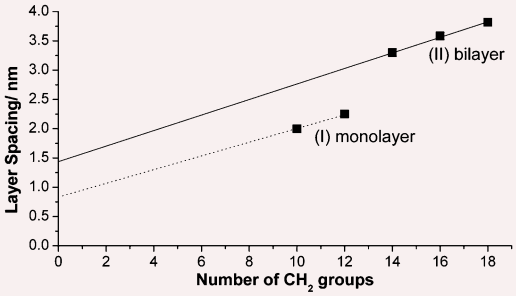

A series of long-chain lamellar hydrated copper(II) alkylsulfonates with different chain molecular assemblies

Seong-Hun Park and Cheol Eui Lee*

Group (I) materials with smaller carbon numbers are composed of interdigitated alkyl chains, whereas group (II) materials are of a non-interdigitated bilayer structure.

1840

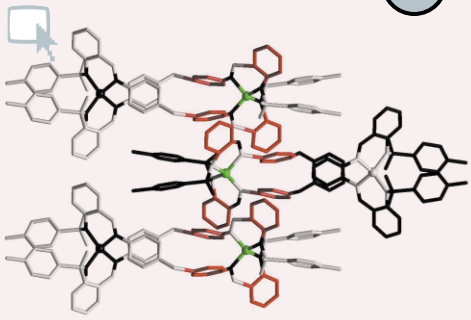

A 3D network of helicates fully assembled by π-stacking interactions

Miguel Vázquez, Angelo Taglietti, Dante Gatteschi,* Lorenzo Sorace, Claudio Sangregorio, Ana M. González, Marcelino Maneiro, Rosa M. Pedrido and Manuel R. Bermejo*

The reported neutral dihelicate forms a unique 3D network in the solid state due to π-stacking interactions, which are responsible for intermolecular antiferromagnetic coupling between Cu(II) ions: this phenomenon is reported for the first time for this class of supramolecular arrays.

1842

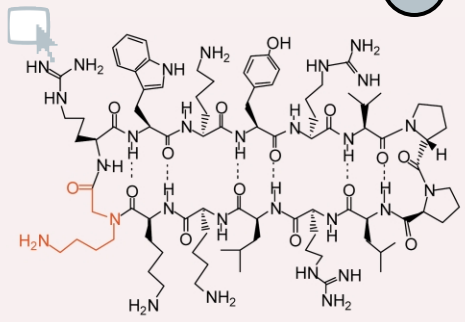

A family of macrocyclic antibiotics with a mixed peptide–peptoid ß-hairpin backbone conformation

Sasalu C. Shankaramma, Kerstin Moehle, Sonya James, Jan W. Vrijbloed, Daniel Obrecht and John A. Robinson*

Novel cationic, macrocyclic peptidomimetics are described that adopt a stable ß-hairpin conformation in aqueous solution, and show antimicrobial activity against Gram +ve and Gram −ve bacteria.

1844

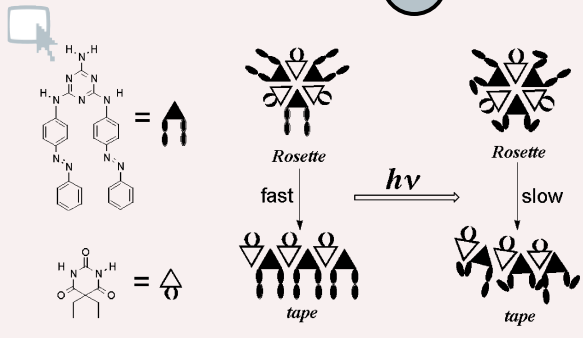

Photoresponsive melamine·barbiturate hydrogen-bonded assembly

Shiki Yagai,* Takashi Karatsu and Akihide Kitamura*

Hydrogen-bonded assembly between a melamine–azobenzene conjugate and barbiturate is reported. In $CHCl_3$, transformation of the soluble *rosette* assemblies into the insoluble *tapelike* assemblies was suppressed drastically *via* photoisomerization of azobenzene units.

1856

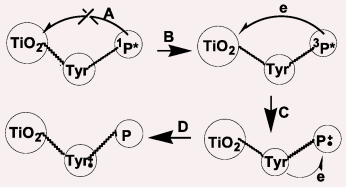

Porphyrin capped TiO_2 nanoclusters, tyrosine methyl ester enhanced electron transfer

Junhua Yu, Jingrong Chen, Xuesong Wang,* Baowen Zhang* and Yi Cao

The photoinduced electron transfer between neutral titanium dioxide nanoclusters and porphyrin is enhanced by the bridging of tyrosine methyl ester to the two components.

1858

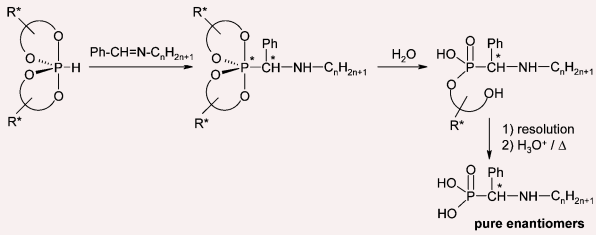

Asymmetric synthesis of (α-amino)phosphonic acid amphiphiles using chiral P–H spirophosphoranes

Christophe Déjugnat, Guita Etemad-Moghadam and Isabelle Rico-Lattes*

Stereoselective addition reaction between chiral P–H spirophosphoranes and long-chain prochiral aldimines affording, after selective hydrolysis, enantiopure (α-amino)phosphonic acid amphiphiles in a monoester or free acid form.

1860

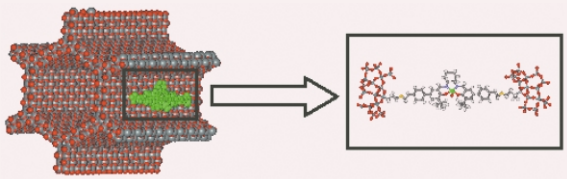

Synthesis and catalytic activity of a chiral periodic mesoporous organosilica (ChiMO)

Carlos Baleizão, Bárbara Gigante,* Debasish Das, Mercedes Alvaro, Hermenegildo Garcia* and Avelino Corma*

Chiral vanadyl salen complex incorporated in the framework of a MCM-41 is active for the enantioselective catalytic addition of cyanotrimethylsilane to aldehydes.

1862

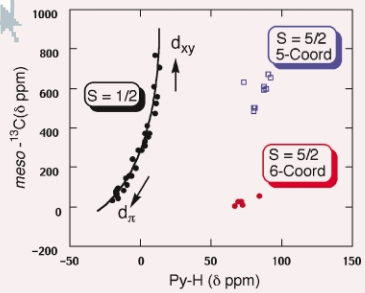

Chemical shift of *meso*-carbon: a powerful probe to determine the coordination structure and electron configuration of ferric porphyrin complexes

Mikio Nakamura,* Akito Hoshino, Akira Ikezaki and Takahisa Ikeue

meso-^{13}C chemical shifts serve as a powerful probe to determine the coordination structure and electron configuration of ferric porphyrin complexes

1864

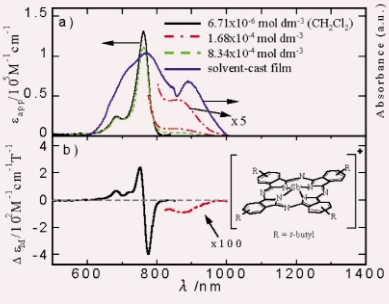

Spectral properties of a novel antimony(III)-phthalocyanine complex that behaves like J-aggregates in non-aqueous media

Hiroaki Isago*

An unusual red-shift of phthalocyanine Q-band upon aggregation in non-aqueous media has been observed for antimony(III) derivative and has been studied by using optical absorption and magnetic circular dichroism spectroscopy.

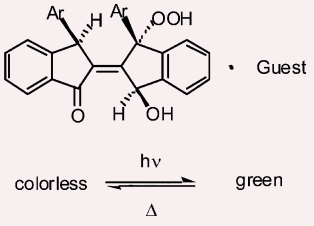

Photochromism of the inclusion crystals of a new hydroperoxybiindenylidene

Koichi Tanaka,* Yohei Yamamoto and Shigeru Ohba

Inclusion crystals of 3,1′-bis(4-fluorophenyl)-1′-hydroperoxy-3′-hydroxy-1′,3′-dihydro-3*H*-[2,2′]biindenyliden-1-one showed photochromic and photomagnetic properties in the solid state.

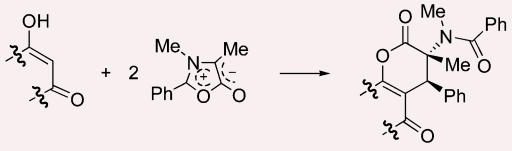

Regio and diastereoselective lactonisation of enolisable 1,3-dicarbonyls by reaction with mesoionic 1,3-oxazolium-5-olates

Giovanni Grassi,* Francesco Risitano, Francesco Foti, Massimiliano Cordaro, Giuseppe Bruno and Francesco Nicolò

Reaction of enolisable 1,3-dicarbonyls and *N*-methyl-1,3-oxazolium-5-olate derivatives provided enol lactones directly in good yield and with excellent regio- and diastereocontrol.

Amidinyl radicals: new and useful intermediates for the synthesis of imidazolines and imidazoles

Dominique Gennet, Samir Z. Zard* and Haiwen Zhang

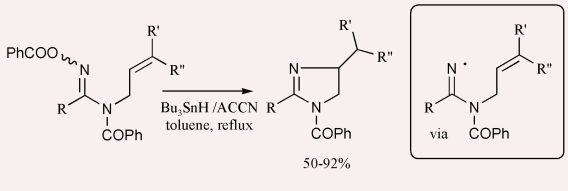

Amidinyl radicals are readily generated from amidoxime benzoates by treatment with a stannane–diazo initiator or with Ni–AcOH and captured by an internal olefin to give the corresponding imidazoline.

Synthesis and biological evaluation of cytostatin analogues

Laurent Bialy* and Herbert Waldmann

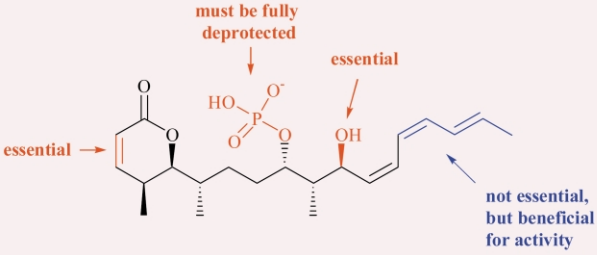

The basic structure–activity relationship (SAR) of PP2A inhibition of the phosphatase inhibitor cytostatin has been derived from the evaluation of a small set of analogues of the natural product.

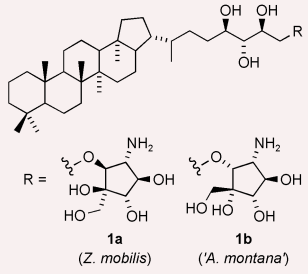

Synthesis of the aminocyclopentitol moieties of the hopanoids of *Zymomonas mobilis* and '*Anacystis montana*'

Jose Luis Chiara,* Isabel Storch de Gracia and Ágatha Bastida

The first synthesis of the cyclopentitol units in bacterial hopanoids **1a** and **1b** has been accomplished from D-glucosamine. The free cyclitol in **1a** shows weak inhibitory activity against α- and β-glucosidases and α- and β-galactosidases.

1876

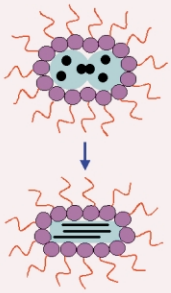

Barium hexaaluminate nanowhiskers synthesized by novel sol–gel process in reverse micellar media

Prashant K. Sahu, B. D. Kulkarni,* R. B. Khomane, S. A. Pardhy, U. D. Phalgune, P. Rajmohanan and Renu Pasricha

Barium hexaaluminate (BHA) synthesized by coupling of sol–gel process in reverse microemulsions shows a unique nanowhisker morphology and high surface area, which are retained after calcination at 1300 °C.

1878

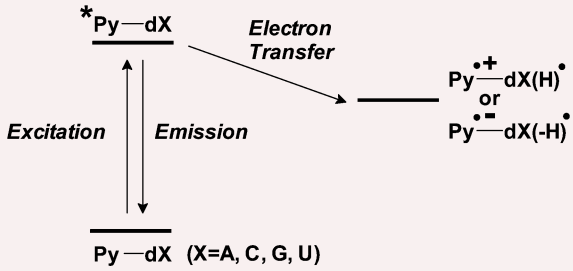

Pyrene as a fluorescent probe for DNA base radicals

Robert Huber, Torsten Fiebig* and Hans-Achim Wagenknecht*

The pH-dependent emission of four pyrene-modified nucleosides provide important information about the acidity or basicity of the DNA base radicals which is relevant to the understanding of charge transport in DNA.

1880

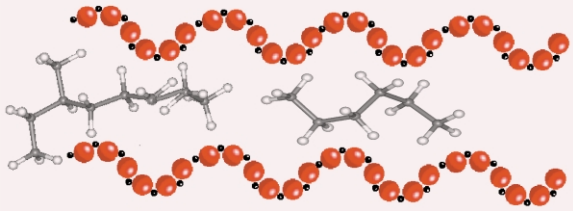

Pore mouth *versus* intracrystalline adsorption of isoalkanes on ZSM-22 and ZSM-23 zeolites under vapour and liquid phase conditions

J. F. Denayer,* A. R. Ocakoglu, W. Huybrechts, J. A. Martens, J. W. Thybaut, G. B. Marin and G. V. Baron

Adsorption experiments reveal that iso-alkanes adsorb only with their linear tail in the pore entrances of ZSM-23 in vapor and liquid phase conditions.

1882

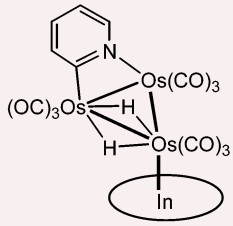

Strong optical limiting capability of a triosmium cluster bonded indium porphyrin complex [(TPP)InOs$_3$(μ-H)$_2$(CO)$_9$(μ-η^2-C$_5$H$_4$N)]

Xinhua Zhong, Yaoyu Feng,* Say-Leong Ong, Jiangyong Hu, Wun-Jern Ng and Zheming Wang

A novel metal–metal bonded indium porphyrin–osmium cluster complex with strong optical limiting capability was first synthesized using the indium porphyrin hydride as precursor and characterized.

1884

A controllable synthetic route to Cu, Cu$_2$O, and CuO nanotubes and nanorods

Minhua Cao, Changwen Hu,* Yonghui Wang, Yihang Guo, Caixin Guo and Enbo Wang

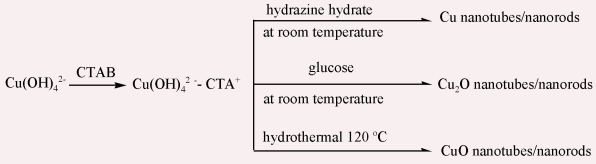

Reducing $Cu(OH)_4^{2-}$ with hydrazine hydrate and glucose in the presence of a structure-directing surfactant at room temperature gave Cu and Cu_2O nanotubes/nanorods, respectively, whereas facile hydrothermal treatment of the $Cu(OH)_4^{2-}$ precursor resulted in CuO nanotubes/nanorods.

Reversed effects of DNA on hydride transfer and electron transfer reactions of acridinium and quinolinium ions

Mari Nishimine, Kei Ohkubo, Takashi Komori and Shunichi Fukuzumi*

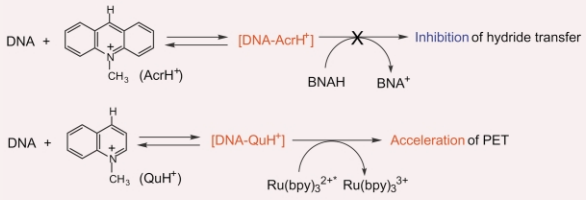

DNA inhibits hydride transfer from 1-benzyl-1,4-dihydronicotinamide to the 10-methylacridinium ion ($AcrH^+$), whereas DNA accelerates photoinduced electron transfer (PET) from the excited state of $Ru(bpy)_3^{2+}$ (bpy = 2,2′-bipyridine) to the 1-methylquinolinium ion (QuH^+).

n-Alkane hydroconversion on Zeogrid and colloidal ZSM-5 assembled from aluminosilicate nanoslabs of MFI framework type

Alexander Aerts, Ward Huybrechts, Sebastien P. B. Kremer, Christine E. A. Kirschhock, Elisabeth Theunissen, Annabel Van Isacker, Joeri F. M. Denayer, Gino V. Baron, Joris W. Thybaut, Guy B. Marin, Pierre A. Jacobs and Johan A. Martens*

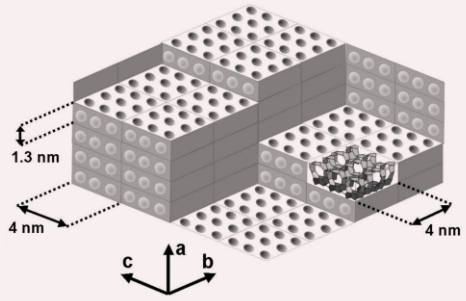

In decane hydroisomerisation, colloidal ZSM-5 and Zeogrid prepared by self-assembly of nanoslabs exhibit molecular shape selectivity different from ZSM-5 obtained by hydrothermal synthesis.

Synthesis of (pyridin-2-yl)hydrazine conjugates as bifunctional chelates using the Suzuki–Miyaura reaction

Jeffrey B. Arterburn,* Bj K. Bryant and DaJun Chen

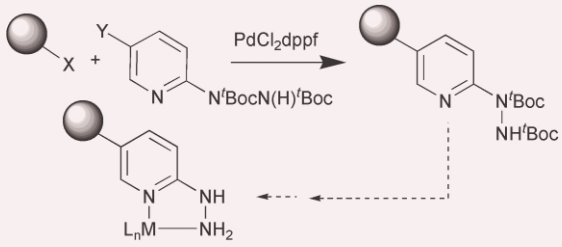

Palladium catalyzed C–C couplings were used to connect (pyridin-2-yl)hydrazine to organic substrates, including a phenylalanine derivative, providing a new method for introducing this important ligand.

Preparation and structures of homoleptic Pu(III) and U(III) acetonitrile salts

Alejandro E. Enriquez, John H. Matonic, Brian L. Scott and Mary P. Neu*

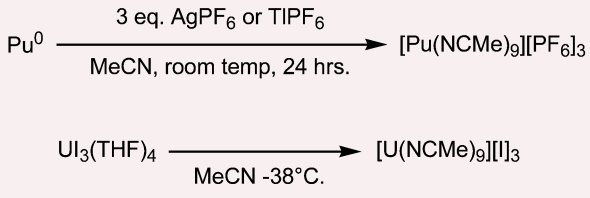

Nine-coordinate homoleptic acetonitrile solvate complexes of Pu(III) and U(III) ions have been prepared through oxidation of Pu metal suspended in acetonitrile with metal-hexafluorophosphate salts and dissolution of $UI_3(THF)_4$ in acetonitrile, respectively.

Trapping volatile nitrosamines with copper incorporated zeolites

Yang Xu, Zhi-yu Yun, Jian Hua Zhu,* Jia-hui Xu, Hua-dao Liu, Yi-lun Wei and Kang-jin Hui

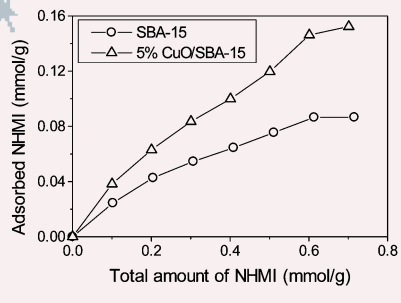

Modification of zeolite or mesoporous materials with copper oxide significantly promotes the selectively adsorption of volatile nitrosamines, beneficial for the removal of nitrosamines in cigarette smoke.

1896

Perchloric acid adsorbed on silica gel as a new, highly efficient, and versatile catalyst for acetylation of phenols, thiols, alcohols, and amines

Asit K. Chakraborti* and Rajesh Gulhane

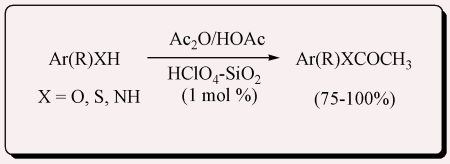

$HClO_4$–SiO_2 efficiently catalyzes the acetylation of phenols, thiols, amines, and alcohols at room temperature under solvent free conditions. Excellent results are obtained during the direct acetylation of alcohols with HOAc.

1898

Immobilized heterobimetallic Ru/Co nanoparticle-catalyzed Pauson–Khand-type reactions in the presence of pyridylmethyl formate

Kang Hyun Park, Seung Uk Son and Young Keun Chung*

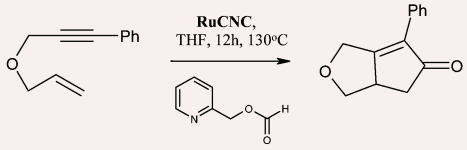

Heterobimetallic Ru/Co nanoparticles immobilized on charcoal were synthesized and used as catalysts in the Pauson–Khand-type reaction in the presence of pyridylmethyl formate instead of carbon monoxide; the catalysts were effective for intra- and intermolecular reactions and easily reused without loss of catalytic activity.

1900

Regioselective hydroxylation of the xylyl linker in a diiron(III) complex having a carboxylate-rich ligand with H_2O_2

Hideki Furutachi, Mizue Murayama, Amane Shiohara, Satoshi Yamazaki, Shuhei Fujinami, Akira Uehara, Masatatsu Suzuki,* Seiji Ogo, Yoshihito Watanabe and Yonezo Maeda

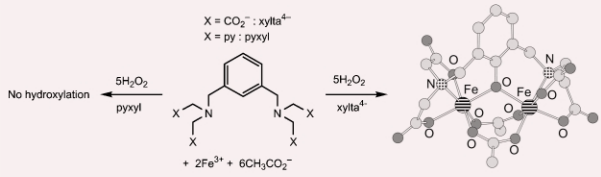

Reaction of a diiron(III) complex having a xylta^{4-} ligand with H_2O_2 resulted in regioselective hydroxylation of the *m*-xylyl linker, mimicking the self-hydroxylation of a phenylalanine sidechain found for R2-W-48F/D84E.

1902

Palladium catalysed [2 + 2 + 1] intramolecular cycloaddition for the preparation of bicyclo[3.3.0]octa-1.5-dien-3-ones from 1,6-diynes

Ronald Grigg,* Lixin Zhang, Simon Collard and Ann Keep

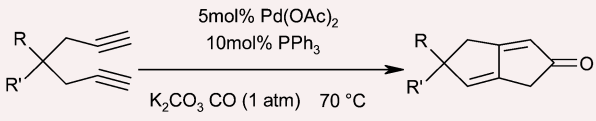

Palladium catalysed [2 + 2 + 1] cycloaddition of 1,6-heptadiynes with CO (1 atm) furnishes bicyclo[3.3.0]octa-1,5-dien-3-ones in 30–74% yield. The use of low pressure carbon monoxide and the high density of functionality in the products make them versatile building blocks for further elaboration.

1904

π-Stacking interactions in some crystalline cisoid *E,E*-1,4-diaryl-1,3-butadienes

Jin Liu,* Elisia M. Murray and Victor G. Young, Jr

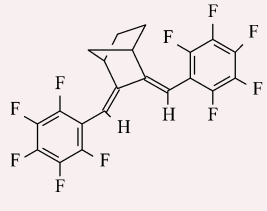

A cisoid *E,E*-1,4-diperfluorophenyl-1,3-butadiene has been prepared in which offset stacking between perfluorophenyl–perfluorophenyl rings occurs, and face-to-face stacking between phenyl–perfluorophenyl rings is found in crystals of its 1 : 1 complex with a cisoid *E,E*-1,4-diphenyl-1,3-butadiene.

1906

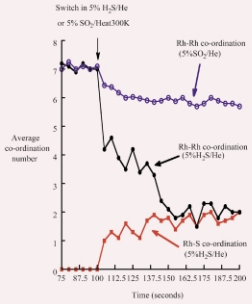

Contrasting dynamic responses of supported Rh nanoparticles to H_2S and SO_2 and subsequent poisoning of NO reduction by H_2

Mark A. Newton,* Andrew J. Dent, Sofia Diaz-Moreno, Steven G. Fiddy, Bhrat Jyoti and John Evans

Dispersive EXAFS delineates the dynamic structural response of supported Rh nanoparticles toward H_2S and SO_2 that underpin the different effects these gases have on selective NO reduction by H_2.

1908

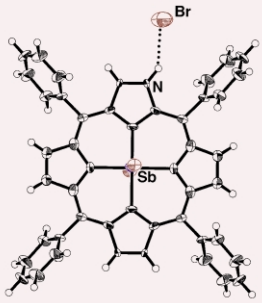

Modulation of axial coordination in N-confused porphyrin–antimony(v) dibromide complex by proton stimulus

Jia-Cheng Liu, Tomoya Ishizuka, Atsuhiro Osuka and Hiroyuki Furuta*

The change of the axial bond length in the antimony(v) N-confused tetraphenylporphyrin dibromide complex was demonstrated by protonation and confirmed from X-ray single crystal analyses.

1910

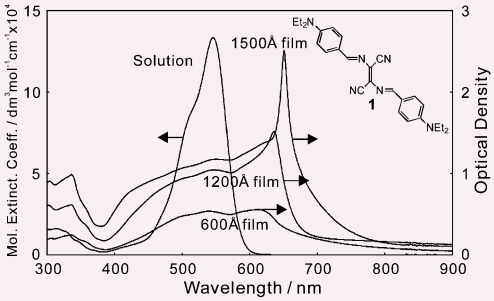

J-Aggregates in vapor deposited films of a bisazomethine dye

Shinya Matsumoto,* Takashi Kobayashi, Tetsuya Aoyama and Tatsuo Wada

This is the first report of J-aggregate formation of a non-ionic bisazomethine dye in vapor deposited films; this dye allows us to prepare easily large homogeneous and very stable J-aggregate thin films and to investigate intrinsic properties of low-dimensional Frenkel excitons.

1912

Highly enantioselective catalytic asymmetric hydrogenation of β-keto esters in room temperature ionic liquids

Helen L. Ngo, Aiguo Hu and Wenbin Lin*

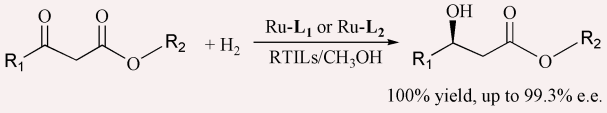

Polar phosphonic acid-derived Ru-BINAP systems were used to catalyze asymmetric hydrogenation of β-keto esters in room temperature ionic liquids (RTILs) with complete conversions and ee values up to 99.3%. The enantioselectivity obtained in RTILs–MeOH is higher than that achieved in MeOH. Both the catalysts and RTILs were recycled *via* simple extraction.

1914

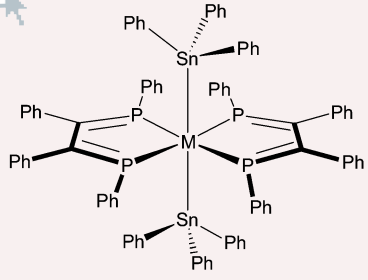

Neutral and dianionic iron and ruthenium 1,4-diphosphabutadiene complexes

Audrey Moores, Nicolas Mézailles, Louis Ricard, François Mathey and Pascal Le Floch*

Synthesis of dianionic iron and ruthenium complexes is reported. These highly reactive species were trapped with Ph_3SnCl to yield the corresponding bis(1,4-diphosphabutadiene) complexes. X-Ray structures are presented.

1916

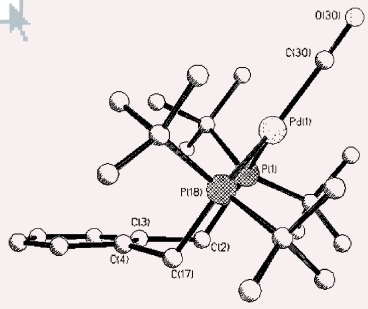

Synthesis, X-ray characterisation and reactions of a trigonal planar palladium(0) carbonyl complex, (tbpx)PdCO

Ronan M. Bellabarba,* Robert P. Tooze and Alexandra M. Z. Slawin

The novel complex (tbpx)PdCO, the first example of a structurally characterised sixteen electron, trigonal planar palladium(0) carbonyl complex, was prepared, characterised by NMR spectroscopy and X-ray crystallography, and some unusual aspects of its reactivity were studied.

1918

A facile aminocyclization for the synthesis of pyrrolidine and piperidine derivatives

Zhihui Shao, Jingbo Chen, Yongqiang Tu, Liang Li and Hongbin Zhang*

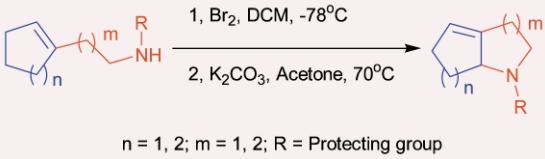

Bromination of an isolated double bond followed by aminocyclization furnishes a highly stereoselective protocol for the intramolecular formation of pyrrolidine and piperidine ring containing subunits that are presented in numerous biologically active natural products.

1920

Novel nanoporous hybrid organic–inorganic silica containing iminodiethanol chelating groups inside the channel pores

Chunqing Liu, Nathaniel Naismith, Lei Fu and James Economy*

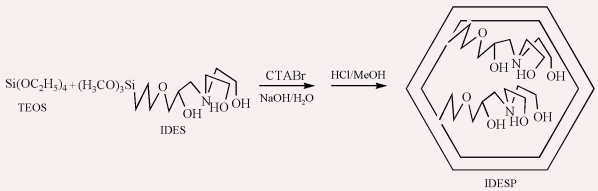

A novel nanoporous hybrid organic–inorganic silica with covalently bound iminodiethanol chelating groups inside the channel pores has been synthesized and is shown to be very efficient in recovery of germanium and antimony oxides from water.

1922

Solid–solid transformation mechanism for nanocrystalline sodalite from pillared clay

Jin–Ho Choy,* Sung-Reol Lee, Yang-Su Han, Man Park and Gyeong-Su Park

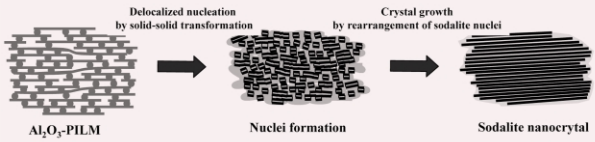

Nanocrystalline sodalite has been synthesized through a solid–solid transformation from a solid gel mixture of Al_2O_3 pillared montmorillonite and hydrated NaOH under mild non-hydrothermal conditions.

1924

Surface effects in the esterification of 9-pyrenebutyric acid within a glass micro reactor

Monica Brivio, R. Edwin Oosterbroek, Willem Verboom,* Martijn H. Goedbloed, Albert van den Berg and David N. Reinhoudt*

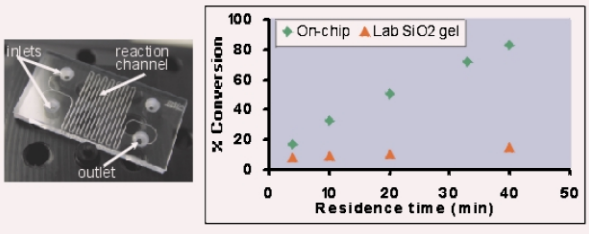

Surface phenomena are an important contribution to the “chip effect”, leading to higher yields and shorter reaction times, as demonstrated for the acid-catalysed esterification of 9-pyrenebutyric acid within a glass fabricated micro reactor.

Observation of high enantioselectivity for the gas phase hydrogenation of methyl pyruvate using supported Pt catalysts pre-modified with cinchonidine

Matthias von Arx, Nicholas Dummer, David J. Willock, Stuart H. Taylor, Richard P. K. Wells, Peter B. Wells and Graham J. Hutchings*

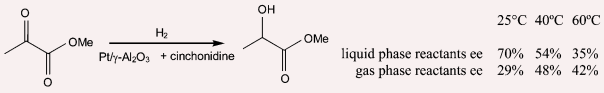

Supported Pt catalysts, pre-modified with cinchonidine, give high ee using gas phase reactants giving the first clear observation of high enantioselection at the gas/solid interface.

A zeolite–enzyme combination for biphasic dynamic kinetic resolution of benzylic alcohols

Stijn Wuyts, Karolien De Temmerman, Dirk De Vos and Pierre Jacobs*

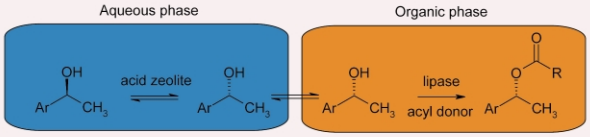

Acid zeolites were found to be very efficient heterogeneous catalysts for racemization of benzylic alcohols in aqueous medium and could be combined in a two-phase system with an enzymatic kinetic resolution resulting in a successful dynamic kinetic resolution (DKR) with a high yield and enantiomeric purity of the resulting product.

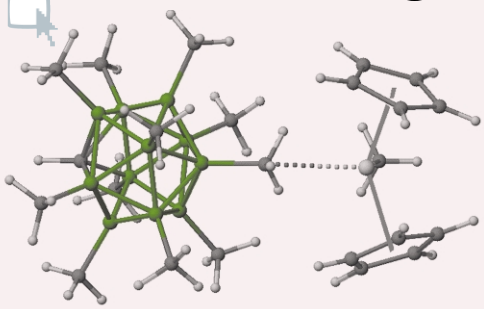

$[Cp_2ZrMe(12\text{-}\mu\text{-}Me\text{-}1\text{-}closo\text{-}CB_{11}HMe_{10})]$: a transition metal complex of a highly-methylated carborane anion

Michael J. Ingleson, Adam Clarke, Mary F. Mahon, Jonathan P. Rourke and Andrew S. Weller*

$[Cp_2ZrMe(12\text{-}\mu\text{-}Me\text{-}1\text{-}closo\text{-}CB_{11}HMe_{10})]$, the first transition metal complex of an highly alkylated carborane anion, is isolated by methide abstraction from Cp_2ZrMe_2 using $[CPh_3][1\text{-}closo\text{-}HCB_{11}Me_{11}]$ and displays a significant intermolecular $Zr\cdots H_3C$ interaction in both the solid state and solution.

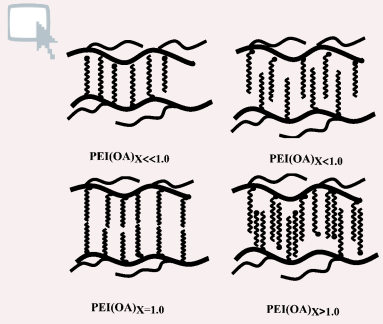

Lamellar architecture and crystalline transformation in supramolecular complexes of highly-branched polyethyleneimine-octadecanoic acid

Surong Zhou, Ying Zhao, Yuanli Cai, Dujin Wang* and Duanfu Xu

Supramolecular complexes of highly-branched polyethyleneimine-octadecanoic acid $PEI(OA)_x$ in the solid state showed typical lamellar structure, and reversible crystalline phase transformation of side alkyl chains was observed with temperature variable FT-IR spectroscopy.

A very efficient, copper-free palladium catalyst for the Sonogashira reaction with aryl halides

Denise Méry, Karine Heuzé and Didier Astruc

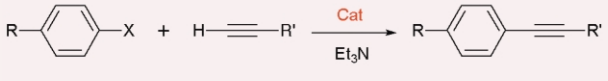

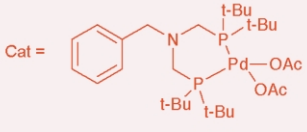

The new electron-rich bis-*tert*-butylphosphine palladium(II) complex represented on the scheme catalyses the Sonogashira reaction between aryl halides with acetylenes at room temperature without co-catalyst.

COMMUNICATIONS

ADDITIONS AND CORRECTIONS

CONFERENCE DIARY

COPIES OF CITED ARTICLES

The Library and Information Centre (LIC) of the RSC offers a first class Document Delivery Service for items in Chemistry and related subjects. Contact the LIC, The Royal Society of Chemistry, Burlington House, Piccadilly, London W1V 0BN, UK.

This service is only available from the LIC in London and not the RSC in Cambridge.

ADVANCE CONTENTS LISTS

Contents lists in advance of publication are available on the web via www.rsc.org/chemcomm – or take advantage of our free e-mail alerting service (www.rsc.org/ej_alert) to receive notification each time a new list becomes available.

ADVANCE ARTICLES AND ELECTRONIC JOURNAL

Free site-wide access to Advance Articles and the electronic form of this journal is provided with a full-rate institutional subscription. See www.rsc.org/ejs for more information.

* Indicates the author for correspondence: see article for contact details.

Electronic supplementary information is available on http://www.rsc.org/esi: see article for further information.

NOTE: An asterisk in the heading of each paper indicates the author who is to receive any correspondence.